Available online at www.sciencedirect.com
SCIENCE DIRECT®
International Journal of Solids and Structures 43 (2006) 1624–1637
INTERNATIONAL JOURNAL OF SOLIDS and STRUCTURES
www.elsevier.com/locate/ijsolstr

Nanoadhesion between a rigid circular disc and an infinite elastic surface

Jiunn-Jong Wu *

Department of Mechanical Engineering, Chinese Culture University, F4, No. 270, Sec. 2, Li-Nong Street, Bei-Tou District, Taipei 112, Taiwan

Received 26 November 2004; received in revised form 8 April 2005
Available online 6 June 2005

Abstract

The adhesion between a nano-scale rigid circular disc and an infinite elastic surface is investigated. By integrating Lennard–Jones potential, the force by the rigid circular disc can be obtained. Then, using the path following method, the load–displacement relationship and pressure distribution are obtained. The proposed method can be extended to the nanoadhesion of other types of bodies.

Keywords: Adhesion; Nanoadhesion; Elastic energy; Lennard–Jones potential

1. Introduction

Nanoadhesion is an important issue in MEMS (microelectromechanical system) (Bhushan, 1999). There exist extensive engineering literatures on various aspects of this field. For example, the adhesion between spheres was investigated by Greenwood (1997) and Feng (2000). The adhesion for elastic beam was investigated by Han et al. (2002).

In this paper, we focus on the adhesion between a nano-scale rigid circular disc and an infinite elastic surface, which is important for micromachines. This is a classical subject, which was investigated by Kendall (1971) and by Persson (2003). Kendal used the energy method, and found the pull-off force. Persson followed Kendall's method, and found the pull-off stress and the critical radius. In his paper, Persson showed that for very small solids the breaking of the adhesive bond will not occur by crack propagation

* Tel.: +886 228610511457; fax: +886 228615241.
E-mail addresses: jjw5277@ms19.hinet.net, jjwu@faculty.pccu.edu.tw

0020-7683/$ - see front matter © 2005 Elsevier Ltd. All rights reserved.
doi:10.1016/j.ijsolstr.2005.04.024

Nomenclature

A	non-dimensional radius of circular disc, $A = a/\varepsilon$
a	radius of circular disc
B	non-dimensional approach of distance, $B = b/\varepsilon$
B_{p}	non-dimensional pull-off distance
b	approach of distance
C_{ij}	element of influence matrix
E	Young's modulus
E^*	equivalent Young's modulus
e	the minimum of the potential
F	pull-off force
$\mathbf{F}$	force vector
f	force on an element of the surface
$\mathbf{f}$, $\mathbf{f}(r,h,a)$	force vector on an element of the surface
$G(H)$, $G_i(H_i)$	equation for Newton–Raphson method
$\mathbf{G}$	inter-surface force kernel (a vector function)
H	non-dimensional distance, $H = h/\varepsilon$
H_A	Hamaker constant
h, $h(r)$	distance between the circular disc and the surface
$K(r)$	the complete elliptic integral of the first kind
$\mathbf{n}_1$, $\mathbf{n}_2$	unit vector normal to surface
P	non-dimensional load, $P = p\varepsilon/\Delta\gamma$
p, $p(r)$	stress
R	non-dimensional coordinate, $R = r/\varepsilon$
r	polar coordinate for infinite surface
S	non-dimensional distance, $S = s/\varepsilon$
S_1, S_2	surface area
s	distance
t	distance
U_{tot}	total energy
$u(r)$	deflection
V_1, V_2	volume
W	non-dimensional load, $W = \Delta\gamma\varepsilon\int p\,\mathrm{d}r$
$w(s)$	potential between two molecules
x	polar coordinate for circular disc
$\mathbf{x}_1$, $\mathbf{x}_2$	vector of the coordinates of a point
z	deformation of the surface
α	a parameter
β	a parameter
$\Delta\gamma$	surface energy
ε	the distance at which $\varepsilon = (\frac{2}{15})^{1/6}\sigma$
μ	parameter, $\mu = (\frac{\Delta\gamma}{E^*\varepsilon^2})^{2/3}$
v	Poisson ratio
ρ_1, ρ_2	the number densities of bodies
σ	the distance at which Lennard–Jones potential is zero
θ	angular coordinate

as is usually the case for macroscopic bodies, but the bond-breaking will be more uniform over the contact area. Both Kendall and Persson did not find the pressure distribution.

In order to find the pressure distribution, we start from the Lennard–Jones potential. By using Argento et al.'s (1997) method, the adhesive force can be obtained. Then, we follow Feng's (2000) method and used Keller's (1977, 1983) method of arc-continuation. The load–displacement relation and pressure distribution can be obtained.

The pull-off force by the current method is compared with Persson's (2003) result. The proposed method can be extended to other problem, such as the adhesion between a nano-sphere and an infinite elastic surface.

2. Mathematical description

The current system is shown in Fig. 1. A circular disc with radius a makes perfect contact with an infinite elastic surface. When a detaching force F is applied to a circular disc, adhesion occurs between the circular disc and the infinite surface.

2.1. Kendall's and Persson's results

When a pulling force F is applied to the disc, the elastic deformation is (Johnson, 1985)

$$z = \frac{F(1-\nu^2)}{2Ea} = \frac{F}{2E^* a} \tag{1}$$

where z is the deformation normal to the surface, E is the Young's modulus, ν is the Poisson ratio, E^* is the equivalent Young's modulus ($E^* = \frac{E}{1-\nu^2}$), and a is the radius of the disc.

Kendall (1971) pointed that total energy is

$$U_{\text{tot}} = -\Delta\gamma\pi a^2 + E^* a z^2$$

The bond-breaking occurs when $\mathrm{d}U_{\text{tot}}/\mathrm{d}a = 0$. Thus, Kendall (1971) found that the pull-off force is

$$F = 2aE^* z = (8\pi a^3 E^* \Delta\gamma)^{1/2} \tag{2}$$

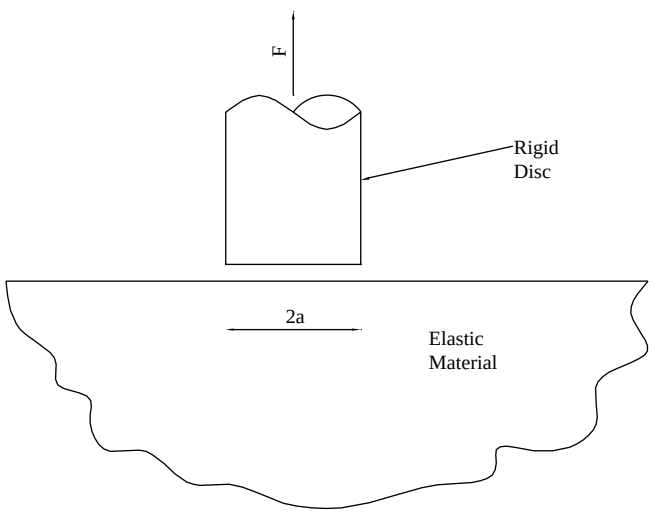

Fig. 1. The adhesion between a rigid disc and an infinite elastic surface.

Persson (2003) found that the relation between the disc radius and the deformation of the surface is

$$a = \frac{E^* z^2}{2\pi\Delta\gamma} \tag{3}$$

Persson (2003) also found that the pull-off stress is

$$p = \left(\frac{8E^*\Delta\gamma}{\pi a}\right)^{1/2} \tag{4}$$

In fact, the pull-off stress is the average stress on the disc, not the stress on the surface. Since Eq. (1) assumes that (Johnson, 1985)

$$p(r) = \frac{F}{2\pi a^2}\left(1 - \frac{r^2}{a^2}\right)^{-1/2} \tag{5}$$

the pressure distribution on the surface should follow Eq. (5).

2.2. Nanoadhesion

When considering the nano-scale adhesion, Derjaguin approximation (1934) is usually used (Greenwood, 1997; Feng, 2000). However, Derjaguin approximation is accurate for smooth convex surfaces with curvature that is small compared to the separation between the bodies (Israelachvili, 1991; Jagota and Argento, 1997). It is not suitable for the current case. Thus, we start from the interaction between molecules.

The interaction between two molecules can be described by Lennard–Jones potential.

$$w(s) = 4e\left[\left(\frac{\sigma}{s}\right)^{12} - \left(\frac{\sigma}{s}\right)^{6}\right] \tag{6}$$

where $w(s)$ is the potential between two molecules (energy), e is the minimum of the potential (energy), σ is the distance at which the potential is zero (length), and s is the distance between two atoms (length).

The force between two bodies can be obtained by integrating Eq. (6) over the volumes. By applying the divergence theorem, the force can be integrated over the surfaces instead (Argento et al., 1997; Jagota and Argento, 1997).

$$\mathbf{F} = \rho_1\rho_2\int_{V_2}\int_{V_1}\nabla_2 w(s)\,\mathrm{d}V_1\,\mathrm{d}V_2 = \rho_1\rho_2\int_{S_2}\int_{S_1}\mathbf{n}_2(\mathbf{G}\cdot\mathbf{n}_1)\,\mathrm{d}S_1\,\mathrm{d}S_2$$

where

$$\mathbf{G} = \frac{(\mathbf{x}_2 - \mathbf{x}_1)}{s^3}\int_s^\infty w(t)t^2\,\mathrm{d}t$$

ρ_1, ρ_2 are the number densities of bodies 1 and 2 (number/volume).

Argento et al. (1997) said that the traction on the surface element of body 1 by the surface of body 2 can be written as

$$\mathbf{f} = \left(\rho_1\rho_2\int_{S_2}\mathbf{n}_2\mathbf{G}\,\mathrm{d}S_2\right)\cdot\mathbf{n}_1$$

Thus, the force acting an element of an infinite surface by a circular disc is

$$\mathbf{f}(r,h,a) = \frac{4e\sigma^6\pi^2\rho_1\rho_2}{3\pi^2\sigma^3}\left\{\frac{\sigma^9}{3}\int_0^a x\,\mathrm{d}x\int_{\theta=0}^{2\pi}(0,0,-1)\frac{h}{(r^2+x^2-2rx\cos\theta+h^2)^6}\,\mathrm{d}\theta\right.$$
$$\left.-\sigma^3\int_0^a x\,\mathrm{d}x\int_{\theta=0}^{2\pi}(0,0,-1)\frac{h}{(r^2+x^2-2rx\cos\theta+h^2)^3}\,\mathrm{d}\theta\right\}$$

where h is the distance between the circular disc and the infinite surface.

Now, we introduce a distance parameter

$$\varepsilon = \left(\frac{2}{15}\right)^{1/6}\sigma$$

For the force and potential between two molecules, zero force and potential occur at σ. But for the force and potential between two infinite surfaces, zero force occurs at ε. In this paper, the circular disc is larger than a molecule, but is smaller than an infinite surface. The zero force should occur at the distance between σ and ε. The result in Section 4 shows that zero force occurs at the distance at ε.

For convenience, another two parameters are introduced. Hamaker constant is (Israelachvili, 1991)

$$H_A = 4e\sigma^6\pi^2\rho_1\rho_2$$

The surface energy is

$$\Delta\gamma = \frac{H_A}{16\pi\varepsilon^2} = \frac{e\sigma^6\pi\rho_1\rho_2}{4\varepsilon^2}$$

Considering the force in z-direction only, the pressure becomes

$$p(s) = \frac{8\Delta\gamma}{3\varepsilon}\left\{\frac{5\varepsilon^9}{\pi}\int_0^a r\,\mathrm{d}r\int_{\theta=0}^{2\pi}\frac{h(s)}{\left[r^2+x^2-2rx\cos\theta+h(s)^2\right]^6}\mathrm{d}\theta - \frac{2\varepsilon^3}{\pi}\int_0^a r\,\mathrm{d}r\int_{\theta=0}^{2\pi}\frac{h(s)}{\left[r^2+x^2-2rx\cos\theta+h(s)^2\right]^3}\mathrm{d}\theta\right\} \tag{7}$$

2.3. Force and deformation

The deflection of a half-space with Young's modulus E and Poisson ratio v under a normal point load p is (Johnson, 1985)

$$u(r) = \frac{p(1-v^2)}{\pi E r} = \frac{p}{\pi E^* r}$$

where $u(r)$ is the deflection and r is the distance from the point load.

For a general axisymmetric pressure distribution $p(r)$, the deflection is

$$u(r) = \frac{4}{\pi E^*}\int_{s=0}^{\infty} p(s)\frac{s}{s+r}K\left(\frac{2\sqrt{rs}}{r+s}\right)\mathrm{d}s$$

where $K(\cdot)$ is an elliptic integral.

The deformation of the surface is

$$z(r) = \frac{4}{\pi E^*}\int_{s=0}^{\infty} p(s)\frac{s}{s+r}K\left(\frac{2\sqrt{rs}}{r+s}\right)\mathrm{d}s$$

where $p(s)$ can be obtained from Eq. (7). The distance between the disc and the surfaces is the original one added by the deformation.

$$h(r) = b + z(r) = b + \frac{4}{\pi E^*}\int_{s=0}^{\infty} p(s)\frac{s}{s+r}K\left(\frac{2\sqrt{rs}}{r+s}\right)\mathrm{d}s \tag{8}$$

where b is the approach of the surfaces. The deformation and pressure of the surface can be obtained by solving Eqs. (7) and (8) simultaneously.

2.4. Non-dimensionalization

Using ε as the characteristic length. We set

$$H=\frac{h}{\varepsilon},\quad B=\frac{b}{\varepsilon},\quad Z=\frac{z}{\varepsilon},\quad \mu=\left(\frac{\Delta\gamma}{E^*\varepsilon}\right)^{2/3}$$
$$R=\frac{r}{\varepsilon},\quad S=\frac{s}{\varepsilon},\quad A=\frac{a}{\varepsilon},\quad P=\frac{p\varepsilon}{\Delta\gamma}$$

where μ is a parameter similar to Tabor's parameter in the contact between two spheres. Eq. (8) becomes

$$H(R)-B+\frac{4\mu^{3/2}}{\pi}\int_{S=0}^{\infty}P(S)\frac{S}{S+R}K\left(\frac{2\sqrt{RS}}{R+S}\right)\mathrm{d}S=0 \tag{9}$$

Eq. (7) becomes

$$P(R)=\frac{8}{3}\left\{\frac{5}{\pi}\int_{X=0}^{A}X\,\mathrm{d}X\int_{\theta=0}^{2\pi}\frac{H(R)}{\left[R^2+X^2-2RX\cos\theta+H(R)^2\right]^6}\mathrm{d}\theta\right.$$
$$\left.-\frac{2}{\pi}\int_{X=0}^{A}X\,\mathrm{d}X\int_{\theta=0}^{2\pi}\frac{H(R)}{\left[R^2+X^2-2RX\cos\theta+H(R)^2\right]^3}\mathrm{d}\theta\right\} \tag{10}$$

The deformation can be obtained by

$$Z=H-B$$

Eqs. (9) and (10) will be solved by Newton–Raphson method and Keller's path following method. By using such a method, the derivative will be used, which is

$$\frac{\mathrm{d}P}{\mathrm{d}H}=\frac{8}{3}\left\{\frac{5}{\pi}\int_{X=0}^{A}X\,\mathrm{d}X\int_{\theta=0}^{2\pi}\frac{1}{\left[R^2+X^2-2RX\cos\theta+H^2\right]^6}\mathrm{d}\theta\right.$$
$$\left.-\frac{2}{\pi}\int_{X=0}^{A}X\,\mathrm{d}X\int_{\theta=0}^{2\pi}\frac{1}{\left[R^2+X^2-2RX\cos\theta+H^2\right]^3}\mathrm{d}\theta\right\}$$
$$+\frac{8}{3}\left\{\frac{5}{\pi}\int_{X=0}^{A}X\,\mathrm{d}X\int_{\theta=0}^{2\pi}\frac{-12H^2}{\left[R^2+X^2-2RX\cos\theta+H^2\right]^7}\mathrm{d}\theta\right.$$
$$\left.-\frac{2}{\pi}\int_{X=0}^{A}X\,\mathrm{d}X\int_{\theta=0}^{2\pi}\frac{-6H^2}{\left[R^2+X^2-2RX\cos\theta+H^2\right]^4}\mathrm{d}\theta\right\} \tag{11}$$

The two-dimensional integration can be reduced into one-dimensional integration, which is shown in Appendix A.

We define a non-dimensional load as

$$W=2\pi\int PR\,\mathrm{d}R=\frac{2\pi}{\varepsilon\Delta\gamma}\int pr\,\mathrm{d}r \tag{12}$$

In terms of the non-dimensional parameter, we replace the deformation Z by the pull-off distance B_p, Eqs. (2)–(4) become

$$W=\frac{2AB_\mathrm{p}}{\mu^{3/2}}=(8\pi A^3)^{1/2}\frac{1}{\mu^{3/4}} \tag{13}$$

$$A = \frac{B_p^2}{2\pi\mu^{3/2}} \tag{14}$$

$$P = \left(\frac{8}{\pi A}\right)^{1/2}\left(\frac{1}{\mu}\right)^{3/4} \tag{15}$$

Eqs. (13)–(15) will be compared with our results.

3. Numerical procedure

3.1. Discretization

We follow Feng's method in the numerical procedure. In order to solve Eq. (9), we define a residue function as

$$G(H) = H(R) - B + \frac{4\mu^{3/2}}{\pi}\int_{S=0}^{\infty} P(S)\frac{S}{S+R}K\left(\frac{2\sqrt{RS}}{R+S}\right)\mathrm{d}S \tag{16}$$

Since the pressure is concentrated in the area $[0, A]$. $[0, 1.5A]$ is large enough for this problem. Eq. (16) is discretized by dividing the one-dimensional domain $[0, 1.5A]$ into a finite number of elements. Each element covers a subdomain confined by two end nodes. In the interval $[R_i, R_{i+1}]$, the unknown H and P are interpolated linearly.

$$H = H_i(1-\xi) + H_{i+1}\xi$$
$$P = P_i(1-\xi) + P_{i+1}\xi$$

Eq. (16) becomes

$$G_i(H_i) = H_i(R_i) - B + \frac{4\mu^{3/2}}{\pi}\int_{S=0}^{\infty} P(S)\frac{S}{S+R_i}K\left(\frac{2\sqrt{R_iS}}{R_i+S}\right)\mathrm{d}S \tag{17}$$

As Greenwood (1997) pointed out, there is a singularity in the elliptic integral Eq. (17) when $R_i = S$. That is, when integrating S over the element $[R_{i-1}, R_i]$ or $[R_i, R_{i+1}]$, the singularity occurs at R_i. On the elements where singular integral occurs, the integral is decomposed into a non-singular part and a singular part. The non-singular part is integrated by Gaussian quadrature. The singular part can be transformed into non-singular two-dimensional integral by using

$$\begin{cases} \int_{\xi=0}^{1} f(\xi)\log\xi\,\mathrm{d}\xi = -\int_{\xi=0}^{1}\int_{\eta=0}^{1} f(\eta\xi)\,\mathrm{d}\eta\,\mathrm{d}\xi \\ \int_{\xi=0}^{1} f(\xi)\log(1-\xi)\,\mathrm{d}\xi = -\int_{\xi=0}^{1}\int_{\eta=0}^{1} f(1-\eta\xi)\,\mathrm{d}\eta\,\mathrm{d}\xi \end{cases}$$

which can be calculated by two-dimensional Gaussian quadrature (Feng, 2000).

Thus, Eq. (17) becomes

$$G_i(H_i) = H_i - B + \mu^{3/2}\sum C_{ij}P_j \tag{18}$$

where $G_i(H_i)$ and H_i means the equation and the gap at (R_i).

3.2. Newton–Raphson method and Keller's path following method

Newton–Raphson method is usually used to solving a non-linear equation. Thus, Eq. (18) will be solved by Newton–Raphson method.

As Greenwood (1997) and Feng (2000) pointed out, for the adhesive contact between spheres, the turning point appeared with the S-shaped load–approach curve for large Tabor parameter. We suppose that the turning point may appear for the adhesion between a circular disc and an infinite surface, too. Similar to Feng's work (2000), Keller's method (1977, 1983) of arc-length continuation is used to obtain the solution in continuation around the turning point for the current problem.

4. Results and discussion

For the case in Attard and Parker's paper (1992) ($H_A = 10^{-20}$ J m^{-3}, $\varepsilon = 0.5$ nm, $E^* = 10^{10}$ J m^{-3}), $\mu = 0.003$. For the case in Persson's paper (2003) ($\Delta\gamma = 3$ meV/Å^2, $\varepsilon = 3$ Å, $E^* = 10^{11}$ J m^{-3}), $\mu = 0.0136$. Thus, we choose $\mu = 0.1$, 0.01 and 0.001 for the current problem. As for the radius of the disc, we assume that $a = 10$ nm, 100 nm and 1 μm. If $\varepsilon = 0.5$ nm, $A = 20, 200, 2000$. Therefore, we simulate the nanoadhesion for the following cases:

$$A = 20, 200, 2000$$
$$\mu = 0.001, 0.01, 0.1$$

Totally, nine cases are investigated. We use 601 grids (600 elements) with length $L = 1.5A$.

First of all, the load–approach relation is investigated. From Eq. (13), $W\mu^{3/2}/A$ is linear with pull-off distance B_p. Thus, we plot the figure in B vs. $W\mu^{3/2}/A$. The curves are shown Figs. 2–4. It is found that the shapes of the curves are similar. It is also found that there is S shape for large μ. All the curves show that zeros load occurs at $B = -1$. That is, the zero force occurs at the distance ε.

The pull-off occurs at negative peak value of W (Feng, 2001). We plot the pull-off pressure distribution and profile for some typical cases in Figs. 5–8. There are two types of pressure distributions and deformation distribution. For large A and μ, the deformation is nearly uniform in the contact area. But the adhesion pressure is not uniform, and does not follow Eq. (5), either. The edge of the flattened area coincides well

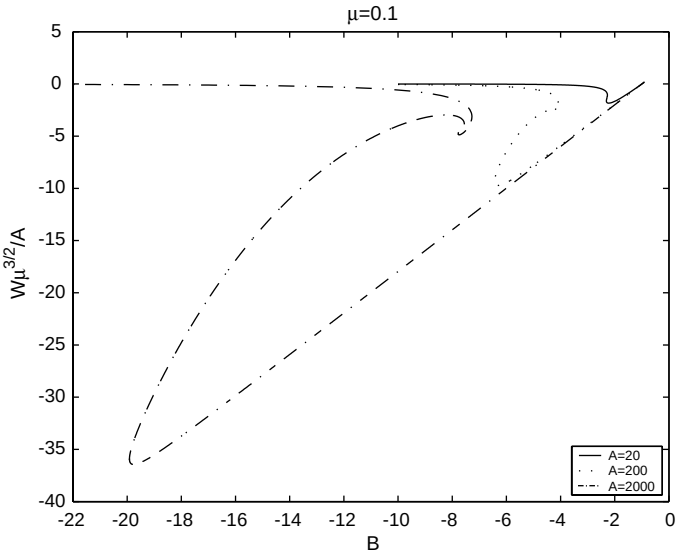

Fig. 2. $W\mu^{3/2}/A$ vs. H curve for $\mu = 0.1$.

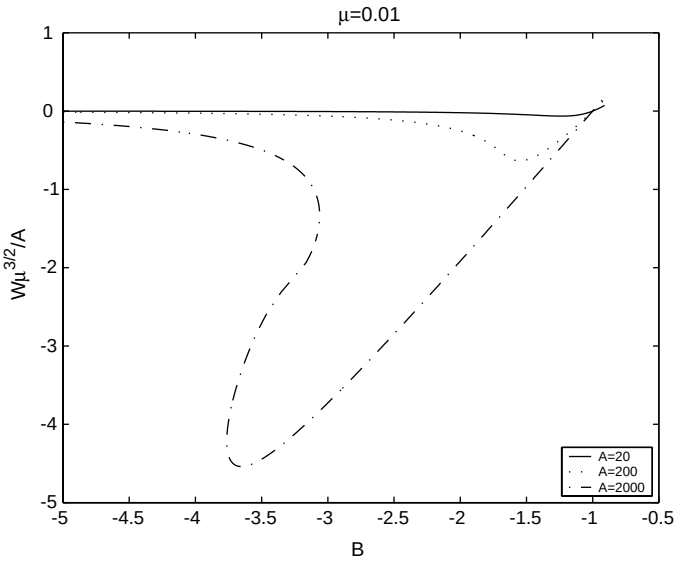

Fig. 3. $W\mu^{3/2}/A$ vs. H curve for $\mu = 0.01$.

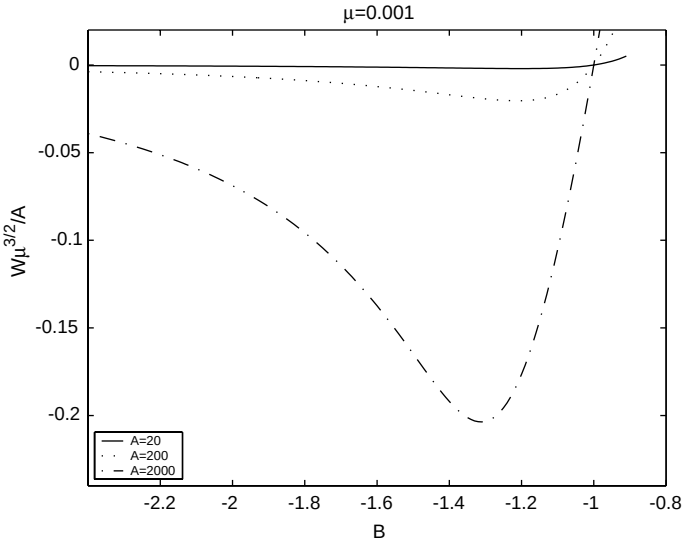

Fig. 4. $W\mu^{3/2}/A$ vs. H curve for $\mu = 0.001$.

with the point where the tensile stress reaches its peaks (Feng, 2000, 2001). At such cases, we can define the edge of contact radius as the maximum adhesion occurs. For these cases, we also find that the contact radius is larger as A and μ are larger.

For small A and μ, the adhesion force is nearly uniform in the contact area. But the deformation is very small, and is not uniform. For these cases, it seems no adhesion happens at all. It is difficult to define the

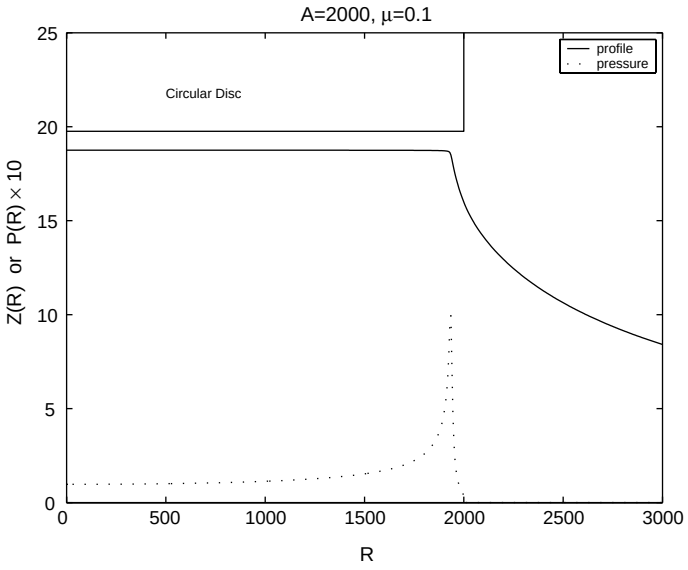

Fig. 5. Profile and pressure for $\mu = 0.1$ and $A = 2000$.

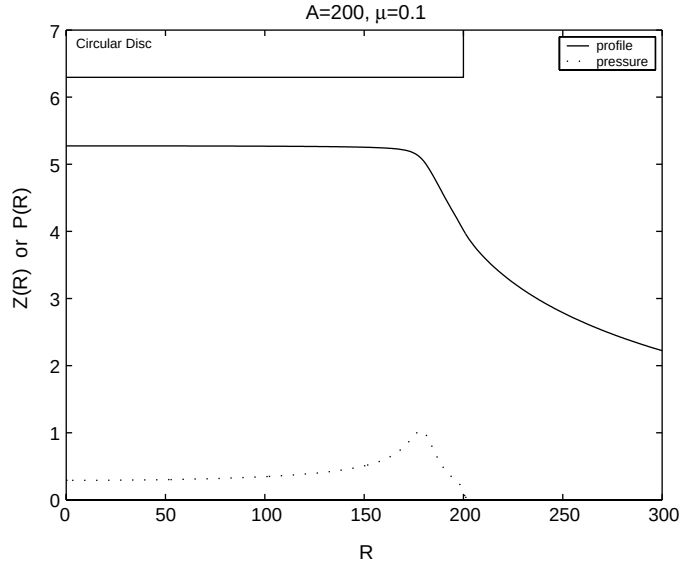

Fig. 6. Profile and pressure for $\mu = 0.1$ and $A = 200$.

contact radius. At the current research, we define the edge of the contact radius as the location where the pressure is 95% of the maximum pressure. Thus, the contact radius is nearly equal to A.

Fig. 9 shows pull-off distance B_p vs. μ for different A. It is shown that Eq. (14) overestimate the pull-off distance B_p for small A and μ. That is, the pull-off distance is less than expected. And for $\mu = 0.001$, the pull-off distance is too small to be estimated.

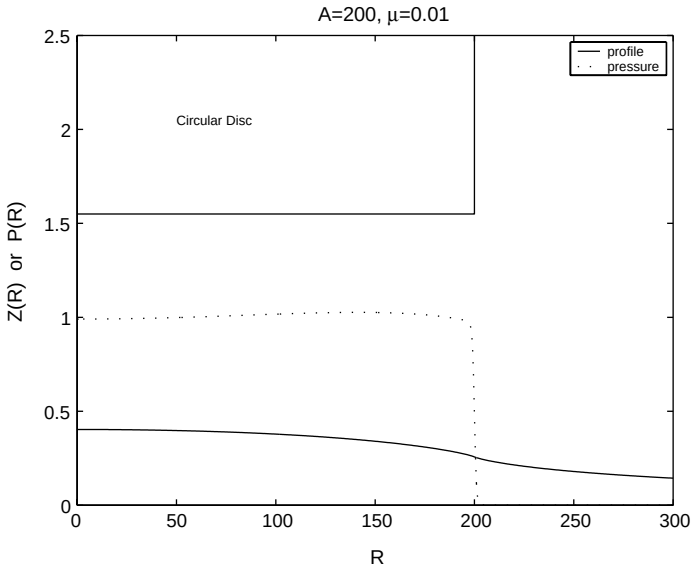

Fig. 7. Profile and pressure for $\mu = 0.01$ and $A = 200$.

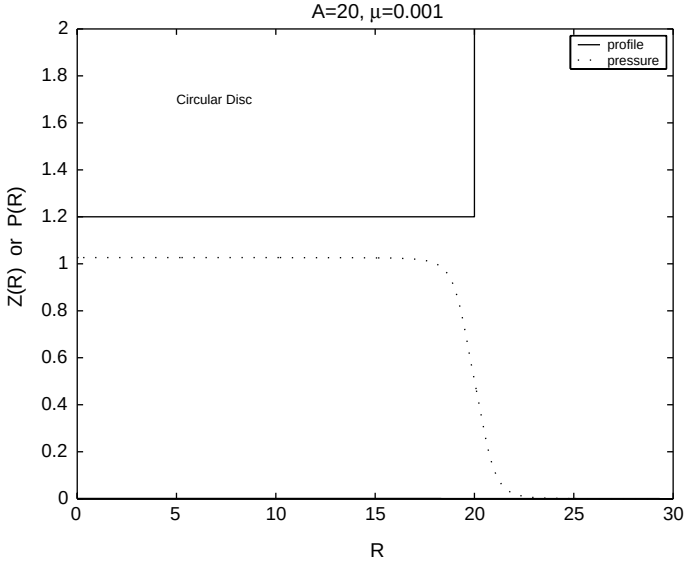

Fig. 8. Profile and pressure for $\mu = 0.001$ and $A = 20$.

Fig. 10 shows A vs. W for different μ. It is shown that Eq. (13) overestimate the pressure for small A and μ. Eq. (13) can predict W only for $\mu = 0.1$.

From Figs. 9 and 10, it shows that Persson's result can predict the nanoadhesion only for $\mu = 0.1$. That is, if the surface is too hard or the surface energy is too small, Eqs. (13)–(15) do not work well.

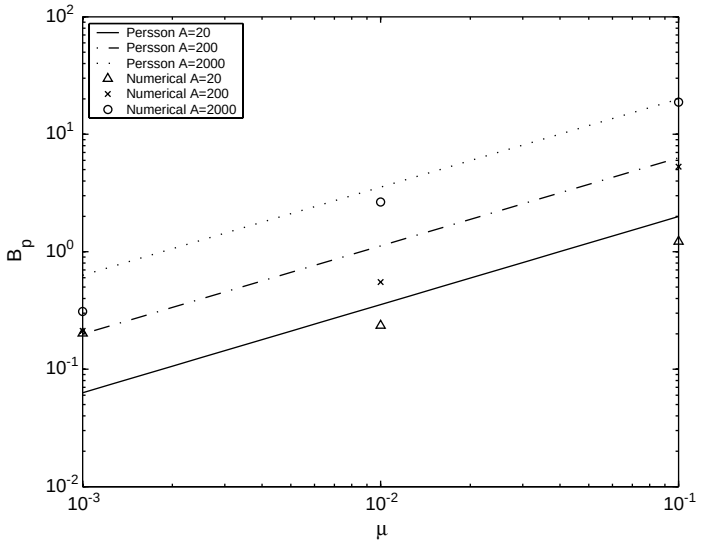

Fig. 9. H vs. μ.

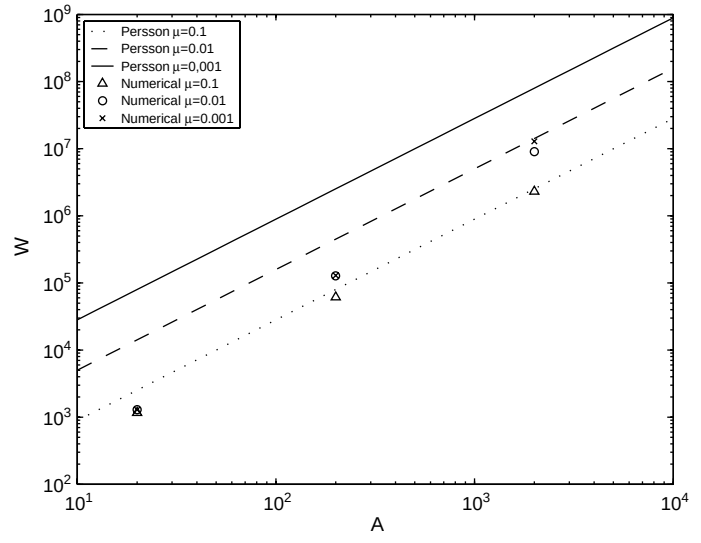

Fig. 10. W vs. A.

5. Conclusion

A numerical method for the adhesion between a circular disc and an infinite elastic surface is proposed. By integrating Lennard–Jones potential, the force by the rigid circular disc can be obtained. Then, using Newton–Raphson method and Keller's path following method, the load–displacement relationship and pressure distribution are obtained. The results show that Persson's prediction (2003) does not work well for small μ.

The current method can be extended to other types of bodies, such as the nanoadhesion between sphere and an infinite elastic surface. Also based on the calculation proposed in this paper, we can test if the bond-breaking will be more uniform when the condition derived by Persson (2003) is satisfied.

Acknowledgments

This research was supported by the National Science Council, Taiwan (NSC 92-2212-E-034-001). The author also thanks the National Center for High-Performance Computing, Taiwan for providing the computer facility.

Appendix A

For $\alpha > \beta$,

$$\int_{\theta=0}^{2\pi} \frac{\mathrm{d}\theta}{(\alpha+\beta\cos\theta)} = \frac{2\pi}{\sqrt{\alpha^2-\beta^2}}$$

For $n \geqslant 1$ and $\alpha > \beta$,

$$\int_{\theta=0}^{2\pi} \frac{\mathrm{d}\theta}{(\alpha+\beta\cos\theta)^{n+1}} = \frac{(2n-1)\alpha}{n(\alpha^2-\beta^2)} \int_{\theta=0}^{2\pi} \frac{\mathrm{d}\theta}{(\alpha+\beta\cos\theta)^{n}} - \frac{(n-1)}{n(\alpha^2-\beta^2)} \int_{\theta=0}^{2\pi} \frac{\mathrm{d}\theta}{(\alpha+\beta\cos\theta)^{n-1}}$$

Set

$$K_n = \int_{\theta=0}^{2\pi} \frac{\mathrm{d}\theta}{(\alpha+\beta\cos\theta)^{n}}$$

Then,

$$K_1 = \frac{2\pi}{\sqrt{\alpha^2-\beta^2}}$$

$$K_{n+1} = \frac{(2n-1)\alpha}{n(\alpha^2-\beta^2)} K_n - \frac{n-1}{n(\alpha^2-\beta^2)} K_{n-1} \quad \text{for } n \geqslant 1$$

All K_n can be obtained recursively.

We need to integrate Eqs. (10) and (11). Thus, set

$$\alpha = R^2 + X^2 + H^2$$
$$\beta = -2RX$$

Then,

$$P(R) = \frac{8}{3}\left\{\frac{1}{\pi}\int_{X=0}^{A} (5K_6 - 2K_3) H(R) X \,\mathrm{d}X\right\}$$

$$\frac{\mathrm{d}P}{\mathrm{d}H} = \frac{8}{3}\left\{\frac{1}{\pi}\int_{X=0}^{A} (5K_6 - 2K_3 - 60K_7H^2 + 12K_6H^2) X \,\mathrm{d}X\right\}$$

The two-dimensional integration is reduced into a one-dimensional integration, which can be calculated by using Gaussian quadrature.

References

Argento, C., Jagota, A., Carter, W.C., 1997. Surface formulation for molecular interactions of macroscopic bodies. Journal of the Mechanics and Physics of Solids 45 (7), 1161–1183.

Attard, P., Parker, J.L., 1992. Deformation and adhesion of elastic bodies in contact. Physical Review A 46 (12), 7959–7971.

Bhushan, B. (Ed.), 1999. Handbook of Micro/nano Tribology, second ed. CRC Press, London.

Derjaguin, B.V., 1934. Untersuchungen uber die reibung und adhasion. IV. Theorie des anhaftens kleiner teilchen. Kolloid Z. 69, 155–164.

Feng, J.Q., 2000. Contact behavior of spherical elastic particles: A computational study of particle adhesion and deformations. Colloids and Surfaces A: Physicochemical and Engineering Aspects 172, 175–198.

Feng, J.Q., 2001. Adhesive contact of elastically deformable spheres: A computational study of pull-off force and contact radius. Journal of Colloid and Interface Science 238, 318–323.

Greenwood, J.A., 1997. Adhesion of elastic spheres. Proceedings of the Royal Society of London A 453, 1277–1297.

Han, W., Kuttler, K.L., Shillor, M., Sofonea, M., 2002. Elastic beam in adhesive contact. International Journal of Solids and Structures 39, 1145–1164.

Israelachvili, J., 1991. Intermolecular and Surface Forces. Academic Press, London.

Jagota, A., Argento, C., 1997. An intersurface stress tensor. Journal of Colloid and Interface Science 191, 326–336.

Johnson, K.L., 1985. Contact Mechanics. Cambridge University Press, Cambridge.

Keller, H.B., 1977. Numerical solution of bifurcation and non-linear eigenvalue problems. In: Rabinowitz, P. (Ed.), Applications of Bifurcation Theory. Academic Press, New York, pp. 359–384.

Keller, H.B., 1983. The bordering algorithm and path following near singular points of high nullity. SIAM Journal on Scientific and Statistical Computing 4 (4), 573–582.

Kendall, K., 1971. The adhesion and surface energy of elastic solids. Journal of Physics D: Applied Physics 4, 1186–1195.

Persson, B.N.J., 2003. Nanoadhesion. Wear 254, 832–834.